Fe^{3+} defect dipole centers in ferroelectric $PbTiO_3$ studied using electron paramagnetic resonance

D. J. Keeble,[1,*] M. Loyo-Menoyo,[1] Z. I. Y. Booq,[1] R. R. Garipov,[1] V. V. Eremkin,[2] and V. Smotrakov[2]
[1]*Carnegie Laboratory of Physics, School of Engineering, Physics, and Mathematics, University of Dundee, Dundee DD1 4HN, United Kingdom*
[2]*Institute of Physics, Rostov State University, Rostov on Don 344090, Russia*
(Received 30 April 2009; published 1 July 2009)

Three Fe^{3+} centers with tetragonal symmetry and with the defect axis parallel to the polarization direction were detected in ferroelectric $PbTiO_3$ crystals using electron paramagnetic resonance. All exhibit large zero-field splittings (ZFS). Two are assigned to Fe^{3+}-oxygen vacancy dipole defect complexes, and the third to the isolated Fe^{3+} with distant charge compensation. The Fe^{3+}-V_O defect with the largest ZFS converts to the second stable center on annealing; comparison of the cubic ZFS terms show the in-plane oxygen ligands relax outwards in stable center.

DOI: 10.1103/PhysRevB.80.014101 PACS number(s): 77.84.Dy, 61.72.J−, 76.30.Fc

I. INTRODUCTION

Point defects and impurities in ferroelectric perovskite oxides, ABO_3, can effect the polarization and pin ferroelectric domain walls, and are assumed to be involved in the atomic mechanisms responsible for aging and fatigue.[1–4] Point defect complexes with a dipole moment, for example a substitutional acceptor impurity with a nearest-neighbor positive oxygen vacancy, are of particular importance.[1–3] It has also been proposed to use defect dipoles to engineer ultrahigh strain materials.[5] Their existence was established in an electron-paramagnetic-resonance (EPR) study of Fe^{3+} in $SrTiO_3$;[6,7] a very large second-order axial zero-field splitting (ZFS) parameter, b_2^0, reflecting a large crystal field, was observed and identified with the Fe^{3+} substituted at the B site with a nearest-neighbor oxygen vacancy, Fe_{Ti}^{3+}-V_O. More recently EPR has observed the alignment of defect dipoles[8,9] and has provided direct insight on fatigue processes.[10]

While there is general agreement on the existence of a large axial zero-field splitting $S=5/2$ center in $PbTiO_3$, normally identified as the Fe_{Ti}^{3+}-V_O complex,[11–15] the results of earlier crystal studies remain uncertain,[12–14] see Table I. The first detailed experiments reported two Fe^{3+} centers with ZFS b_2^0/h values of ~27 and ~16 GHz, respectively.[12] The existence of second center was subsequently questioned in a study which reported two centers with large b_2^0/h values of 34.5 and 35.6 GHz at 85 K.[13] Conflicting interpretations of the Fe^{3+} center EPR in $PbTiO_3$ have resulted.[12–14]

Here EPR measurements on a series of $PbTiO_3$ crystals are reported. Three Fe^{3+} centers were observed, all crystals showed at least one of these, the majority two, and a smaller number all three. Earlier studies are explained and the existence of two types of Fe^{3+}-V_O defect inferred. The center with the largest second-order zero-field splitting is found to convert to the dominant stable dipole defect center with annealing. The third center, with the smallest ZFS, is proposed to be the isolated Fe_{Ti}^{3+} defect, with distance charge compensation, in agreement with an earlier assignment.[12] The measured cubic ZFS terms provide evidence for an outward relaxation of the in-plane OII oxygen ligands in the stable defect dipole center.

The EPR of the $S=5/2$ Fe^{3+} ion is accurately describe using a spin Hamiltonian (SH) that includes both the Zeeman interaction between the electronic spin and the applied magnetic field, B, and zero-field splitting terms,

$$\hat{\mathbf{H}} = \beta_e \mathbf{B} \cdot \mathbf{g} \cdot \hat{\mathbf{S}} + \hat{\mathbf{H}}_{ZFS}. \tag{1}$$

The ZFS terms can be conveniently expressed using extended Stevens spin operators,[16,17] these emphasize the site symmetry described by the relevant Laue-symmetry class of the center. For the 4/mmm class these can be expressed in the form,[18]

$$\hat{\mathbf{H}}_{ZFS} = \tfrac{1}{3} b_2^0 \hat{\mathbf{O}}_2^0 + \tfrac{1}{60} b_4^0 \hat{\mathbf{O}}_4^0 + \tfrac{1}{60} b_4^4 \hat{\mathbf{O}}_4^4. \tag{2}$$

II. EXPERIMENT

Lead titanate crystals from two sources were studied. Samples were grown by a modified flux method at Argonne National Laboratory,[19] most were polydomain, with a majority 180° domains oriented parallel to the crystal c axis perpendicular to the main face. However, detailed measurements were performed using a detwinned crystal (90° domains removed), heat treated under compressive stress and poled with an electric field of 18 kV/cm. Polydomain flux grown crystals from Rostov State University were also studied.

EPR measurements were made in the 9 GHz band using a Bruker EMX spectrometer, with an ER4122SHQ resonator,

TABLE I. Electron-paramagnetic-resonance ZFS parameter values for Fe^{3+} centers in $PbTiO_3$ crystals.

b_2^0/h (GHz)	b_4^0/h (GHz)	b_4^4/h (GHz)	T (K)	Assignment	Ref.
27.0(1.5)			290	Fe_{Ti}^{3+}-V_O	12
33.0(1.5)			77	Fe_{Ti}^{3+}-V_O	12
15.9(6)	0.41(6)	2.0(3)	290	Fe_{Ti}^{3+}	12
35.59(6)	0.13(21)	1.50(52)	85	Fe_{Ti}^{3+}-V_O	13
34.48(9)	0.13(25)	1.65(75)	85		13
27.13(6)	−0.11(12)	4.20(21)	290	Fe_{Ti}^{3+}	14

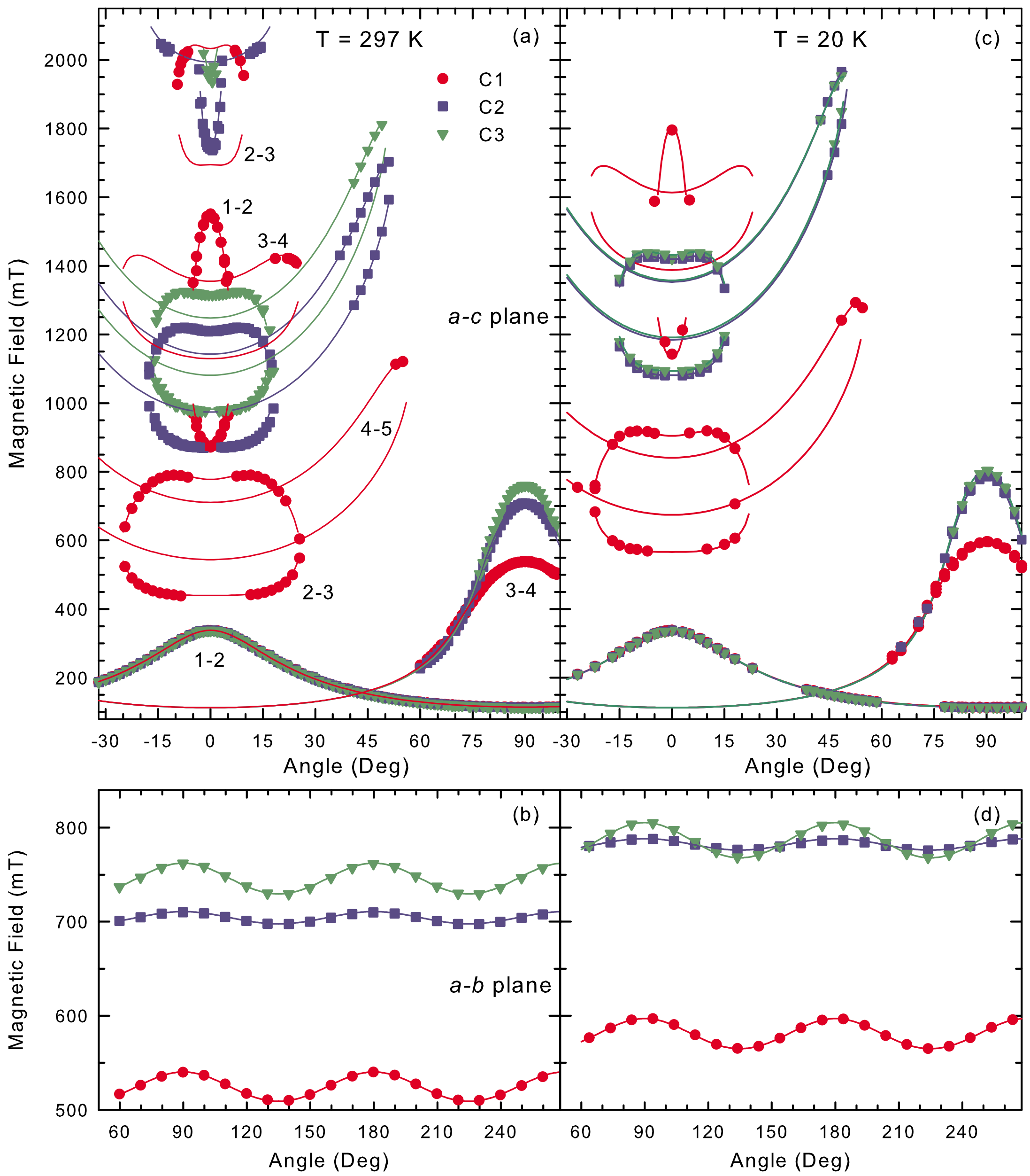

FIG. 1. (Color online) The experimental EPR line position roadmaps, center 1 (circle), center 2 (square), and center 3 (triangle), and the associated lines of best fit using the spin-Hamiltonian parameters given in Table II. (a) room temperature $a-c$ plane, the angle is defined with respect to the crystal c axis, transition labels are shown for center 1, (b) the $a-b$ plane with the angle is given with respect to the perpendicular face normal to the direction defined as the a axis. The 20 K roadmaps are given in (c) and (d).

an automated goniometer, and a 2 T electromagnet calibrated using an NMR magnetometer. Variable temperature measurements used an Oxford ESR900 helium flow cryostat. Spectrum simulations were performed using the package EasySpin.[20] Annealing experiments were carried out using a movable tube furnace connected to a mass spectrometer, the base pressure was better than 1×10^{-2} Pa.

III. RESULTS AND DISCUSSION

The EPR line position roadmaps from the detwinned crystal, taken at 297 and 20 K, are shown in Fig. 1, varying the direction of the applied magnetic field in the $c-a$ and $a-b$ crystal planes, in Figs. 1(a) and 1(c) angles are defined with respect to the c axis which is perpendicular to the main face of the rectangular crystal and in Figs. 1(b) and 1(d) with respect to the normal with one of the two narrow faces. Three Fe^{3+} $S=5/2$ centers with tetragonal site symmetry, and with the C_4 axis parallel to the crystal c axis, were observed. The simulated line positions using the best-fit parameters in Eq. (1) for the three centers are shown in Fig. 1. Transitions involving levels from all three Kramers doublets were observed for each center, see Figs. 1 and 2, in contrast to pre-

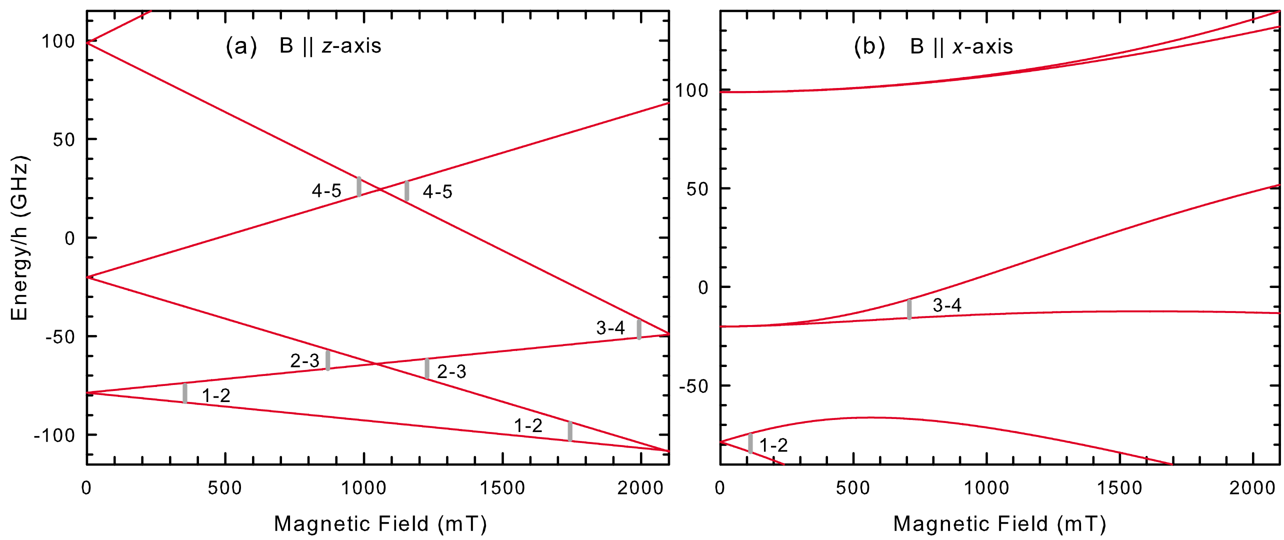

FIG. 2. (Color online) Center 2 energy-level diagrams for magnetic-field B (a) parallel and (b) perpendicular, to the spin-Hamiltonian z axis showing observed transitions.

vious studies. This allowed complete and accurate SH parameters to be determined.

The cubic ZFS term, b_4^4, was directly obtained from the oscillation of transition 2–3 in the $a-b$ plane, see Fig. 1(b). Despite the observation of looping transitions 1–2 and 2–3 up to high field for all centers [Fig. 1(a)] fitting was not able to uniquely determine the values of axial ZFS terms b_2^0 and b_4^0. This ambiguity was removed by the observation, at intermediate angles, of the 4–5 transition loop shown in Fig. 1(a). The dominant axial second-order ZFS term values, b_2^0/h, were found to be 17.46(2), 29.52(3), and 32.49(3) GHz for centers C1, C2, and C3, respectively. The complete ZFS SH for the three centers is given in Table II. The fitted g factors for all centers were found to be near isotropic and temperature independent with a value of 2.005(4). The sign of b_2^0/h was determined to be positive for C2 comparing the room temperature to 5 K intensity ratios.

The EPR spectrum for $B \perp c$, from a multidomain crystal, is shown in Fig. 3(a). For this sample the concentrations ([]) of C3 and C2 are comparable; more typically [C2] was at least a factor two greater that [C3] and C1 was often absent. The total concentration of Fe^{3+} was estimated to be in the range ~20–300 ppm for the crystals studied. Measurements with the detwinned crystal showed that the SH z axis was

TABLE II. Fitted zero-field splitting parameter values at 297 and 20 K.

Center	b_2^0/h (GHz)	b_4^0/h (GHz)	b_4^4/h (GHz)	T (K)	Assignment
1	17.46(2)	0.174(7)	1.74(6)	297	Fe_{Ti}^{3+}
	21.09(2)	0.180(7)	1.86(6)	20	
2	29.52(3)	0.150(7)	0.66(6)	297	Fe_{Ti}^{3+}-V_O
	35.46(3)	0.150(7)	0.66(6)	20	
3	32.49(3)	0.108(7)	1.80(6)	297	Fe_{Ti}^{3+}-V_O
	35.67(3)	0.090(7)	1.98(6)	20	

aligned parallel to the bulk polarization direction for the three centers; no defects with their tetragonal axis perpendicular to the domain axis were detected. It should also be noted that in tetragonal phase of $PbTiO_3$ such defects would have orthorhombic site symmetry, giving additional ZFS terms. The EPR spectra from multidomain crystals showed the presence of ~90° domains by observation of Fe^{3+} centers with their z axes oriented perpendicular to the platelet face.

Large values of b_2^0 are expected for Fe^{3+} in a strong tetragonal field. The influence of ligand-ion geometry surrounding the paramagnetic ion on the values of the EPR ZFS terms can be quantified using the Newman superposition model (NSM).[21] The model assumes that each ligand makes a contribution to the ZFS and that these can be determined using a function that depends only on the separation between the paramagnetic ion and the ligand, R_L, and is intrinsic to the particular ion-ligand pair. The second-order term b_2^0 is calculated using

$$b_2^0 = \sum_L \bar{b}_2(R_L) \tfrac{1}{3}(3\cos^2\theta_L - 1) \tag{3}$$

where polar coordinates (R_L, θ_L, ϕ_L) denote the position of the ligand with respect to the paramagnetic ion and the sum is over all nearest neighbors. The polar coordinates are defined with respect to x, y, z axes that are parallel to the crystal a, b, c axes, but centered on the paramagnetic ion, as shown in Fig. 4. The intrinsic parameters are described by $\bar{b}_k(R_L) = \bar{b}_k(R_0)(R_0/R_L)^{t_k}$, where $\bar{b}_k(R_0)$ and t_k are determined from experiment; typically on a cubic reference material, which also defines the reference distance, R_0. The NSM provides a valuable link between experimental ZFS parameters and ligand geometry.

Ion size arguments support the normal assumption that Fe^{3+} substitution occurs at the B site (Pb^{2+} 163, Ti^{4+} 74.5, and Fe^{3+} 78.5 pm). Applying Eq. (3) and assuming Fe^{3+} is located at the A site was found to give a b_2^0 value nearly two orders too small. Figure 5 shows the calculated b_2^0/h values

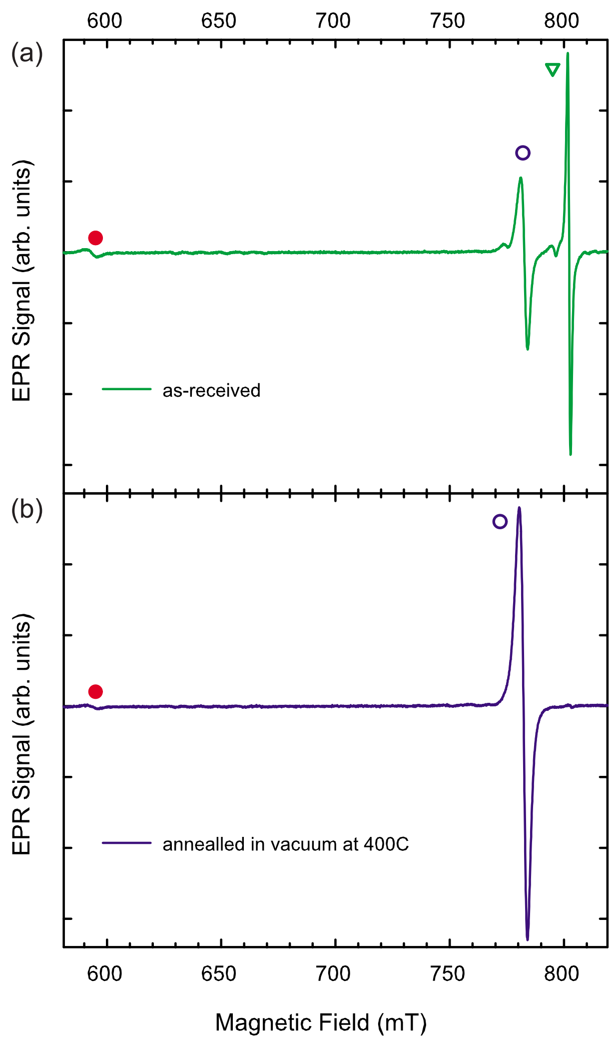

FIG. 3. (Color online) 50 K EPR spectra with B perpendicular to the c axis for a $PbTiO_3$ crystal divided in two (a) as-grown and (b) vacuum anneal ($<1\times10^{-2}$ Pa) at 400 °C for two hours. Symbols denote three Fe^{3+} centers; center 1 (filled circle), center 2 (open circle), and center 3 (triangle).

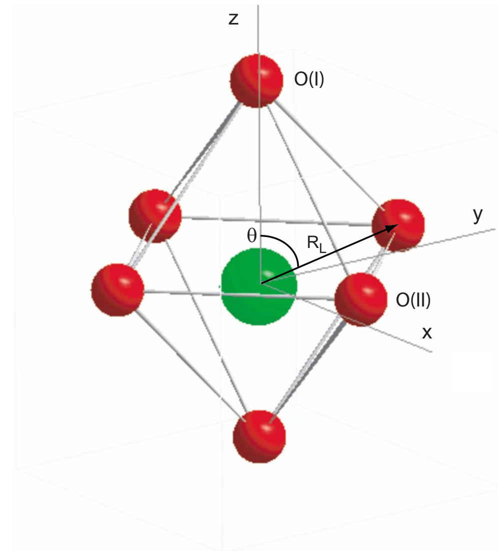

FIG. 4. (Color online) Coordinate system for Newman superposition model (NSM) calculations. The x,y,z axes are parallel to the crystal a,b,c axes, but are centered on the paramagnetic ion. The polar angle θ_L is the angle between the z axis and the particular ion to oxygen ligand vector and the azimuthal angle is the angle in the x,y plane of the projection. Here the ion is shown substituted at the exactly at the Ti position in $PbTiO_3$.

assuming Fe^{3+} substitutes at the Ti-site, or displaced along c axis with and without a nearest-neighbor apical oxygen-vacancy defect. Otherwise perfect lattice ligand positions were assumed.[22] Calculations were performed using two second-order NSM model parameter values derived from pressure dependent EPR studies of Fe^{3+} in MgO and in $SrTiO_3$, and given in Table III. It was assumed the oxygen vacancy was at either the original strong Ti-O position (top right schematic Fig. 5) or the weak bond position (top left schematic Fig. 5). Given this restriction and some uncertainty in the model parameter values, the agreement with experiment is satisfactory. They provide evidence that center 1 is Fe^{3+} substituted on the c axis within a complete oxygen octahedron, the isolated Fe^{3+}_{Ti} center, and that centers 2 and 3 both involve an apical oxygen vacancy. The assignment of center 1 to the isolated Fe^{3+}_{Ti} was suggested earlier,[12] but subsequently disputed.[13,14] Fig. 5 also supports the expectation that the local charge imbalance will tend to move the impurity ion off the Ti-site toward the center of the oxygen (OII) $a-b$ plane.[3,23] However, it should be noted that the uncertainties in the model parameter values (Table III) and the local structure preclude the level of precession reported in recent calculations for the Fe^{3+}_{Ti}-V_O center in $PbTiO_3$.[23]

The fourth-order cubic term b_4^4 values for centers 1 and 3 were found to be similar, 1.80 and 1.74 GHz, respectively, however, the center 2 value, 0.66 GHz, is significantly smaller. The superposition model expression for calculating this term is,

$$b_4^4 = \sum_L \bar{b}_4(R_L)\tfrac{35}{8}\sin^4\theta_L \cos 4\phi_L. \tag{4}$$

It shows that the value of b_4^4 is sensitive to the $a-b$ plane OII ligand positions, but is insensitive to the presence (or absence) of the apical oxygen ligands (Fig. 4). Calculations using the undistorted octahedron and the intrinsic parameters derived from MgO and from $SrTiO_3$ (Table III) were made with a range of commonly used t_4 values (10 to 18) and are shown in Fig. 6. The calculated b_4^4 values spanned experiment for centers 1 and 3, but were greater than the center 2 value. The expected weak dependence on displacements along the c axis was confirmed, a 32 pm displacement of the Fe^{3+} ion from the Ti-site to the center of the OII plane decreased b_4^4 by $\sim$15–18%. However, a 4 pm outward relaxation of the OII ion positions causes a $\sim$21–24% reduction. The similarity of experimental b_4^4 values for centers 1 and 3 suggest similar OII positions. The $\sim$60% smaller value observed for the dominant Fe^{3+}_{Ti}-V_O defect, center two, provides evidence that the $a-b$ plane OII ligands relax outwards.

To gain further insight on the relationship between the three centers annealing studies were performed. Figure 3 shows the results for a crystal divided into two, one piece

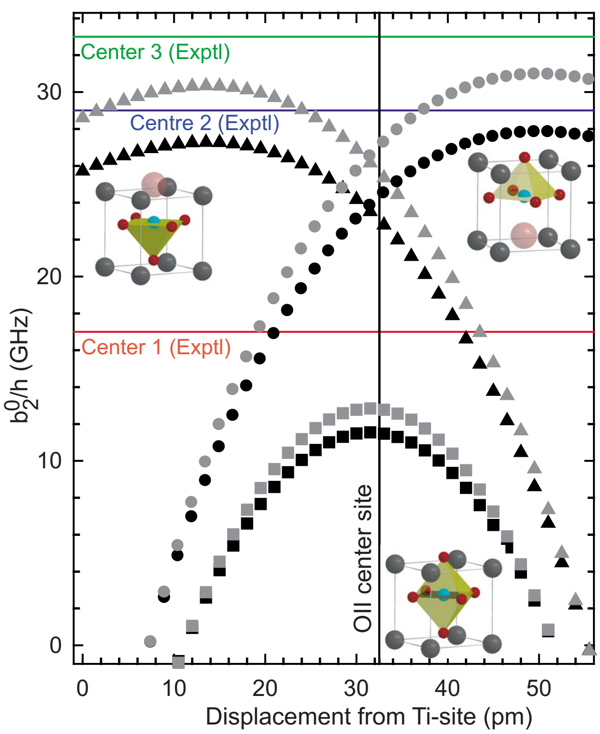

FIG. 5. (Color online) NSM calculations of the axial second-order ZFS term as a function of Fe^{3+} ion displacement along the c axis from the Ti-site position. The isolated Fe^{3+} (square), shown in the bottom schematic, V_O in weak bond site (triangle), top left schematic, and V_O in strong bond site (circle), top right schematic. NSM parameters derived from MgO (gray) and from $SrTiO_3$ (black).

was then annealed at 400 °C in vacuum ($<1\times10^{-2}$ Pa) for two hours. Center 3 was eliminated and a concomitant increase in the intensity of center 2 observed. Further experiments showed that a 30 min anneal in $\sim1\times10^{-1}$ Pa at 290 °C was sufficient to make the conversion. The concentration of center 1 decreased by ~15–20% after the vacuum anneal, possibly due to the partial conversion of isolated Fe_{Ti}^{3+} to Fe_{Ti}^{3+}-V_O resulting from isolated oxygen-vacancy migration.

The dominant Fe_{Ti}^{3+}-V_O ($b_2^0/h=29.52$ GHz) has been seen in all previous EPR studies of crystal and powder $PbTiO_3$.[12–15] First-principles calculations of impurity-ion oxygen-vacancy complexes in $PbTiO_3$ provide evidence that the most stable position for the oxygen vacancy is at the short, strong, bond apical site (top right schematic in Fig. 5).[3,23] It has been suggested that while the defect dipole is parallel to the bulk polarization for this configuration, the distortion of the surrounding alternating weak strong Ti–O c-axis bonds gives a net local polarization in the opposite direction.[3] Both studies also predict that the impurity ion will displace, along the c axis, away from the oxygen vacancy to a position close to the OII oxygen plane. The SH ZFS term b_4^4 values measured here provide evidence that these oxygen positions also relax.

TABLE III. Superposition model parameter values for Fe^{3+} with oxygen ligands.

Host	R_0 (pm)	$\bar{b}_2/h$ (GHz)	t_2	Ref.	$\bar{b}_4/h$ (MHz)	Ref.
MgO	210.1	−12.35(75)	8(1)	7	87.8(1)	25
$SrTiO_3$	195.2	−20(3)	8(1)	7	84.9(1.4)	26

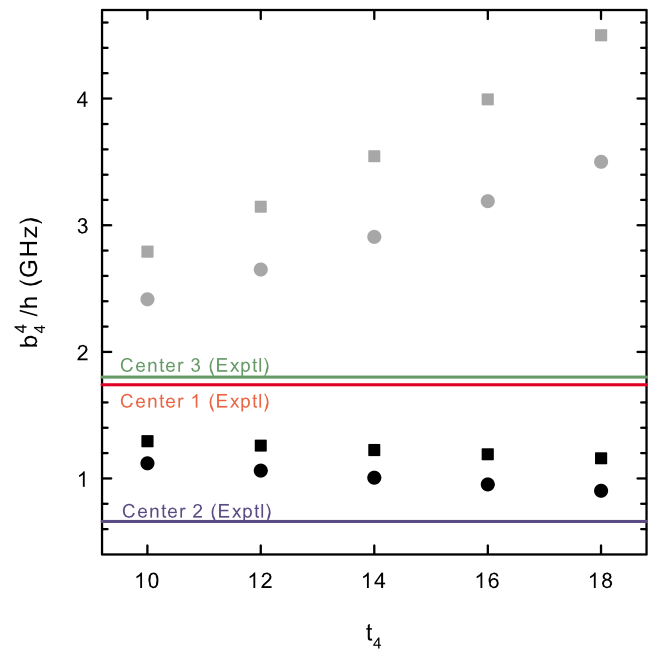

FIG. 6. (Color online) NSM calculations of the cubic fourth-order ZFS term for Fe^{3+} substituted at Ti-site (circle) and the center of OII plane (square). NSM parameters derived from MgO (gray) and from $SrTiO_3$ (black).

The metastable Fe_{Ti}^{3+}-V_O defect, center 3, showed the largest b_2^0/h value, 32.49 GHz. The b_4^4 value is comparable to the that for Fe_{Ti}^{3+}, center 1, suggesting similar OII positions. It has also been observed that EPR linewidths for center 3 are significantly narrower than for centers 1 and 2;[13] from Fig. 3 these are 1.25(5), 4.5(2), and 3.0(2) mT, respectively. The dominant contribution to the linewidth is expected to be unresolved ^{207}Pb near-neighbor superhyperfine structure (SHFS).

It has recently been proposed that Fe^{3+}-V_O-Fe^{3+} defects may be stable[23] and would explain the low [Fe_{Ti}^{3+}] without the need for additional acceptor defects. However, this should result in an EPR spectrum with two markedly different Fe^{3+} signals with strong dipolar coupling.[23] If the complexes could be dissociated an increase in both [Fe_{Ti}^{3+}-V_O] and [Fe_{Ti}^{3+}] would be expected, inconsistent with the annealing results. An alternative model would be an Fe_{Ti}^{3+}-V_O defect to which an additional impurity ion was bound, for example a proton that could be released on annealing. The binding of H would seem attractive given the low anneal temperature required to convert the defect to the stable Fe_{Ti}^{3+}-V_O configuration. The narrower linewidth could result from a suppression of the transferred SHF interactions via the oxygen ligands due to the presence of the impurity. However, first-principles calculations suggest hydrogen may prefer to bond to one of the OII oxygens,[24] this would lower the observed tetragonal

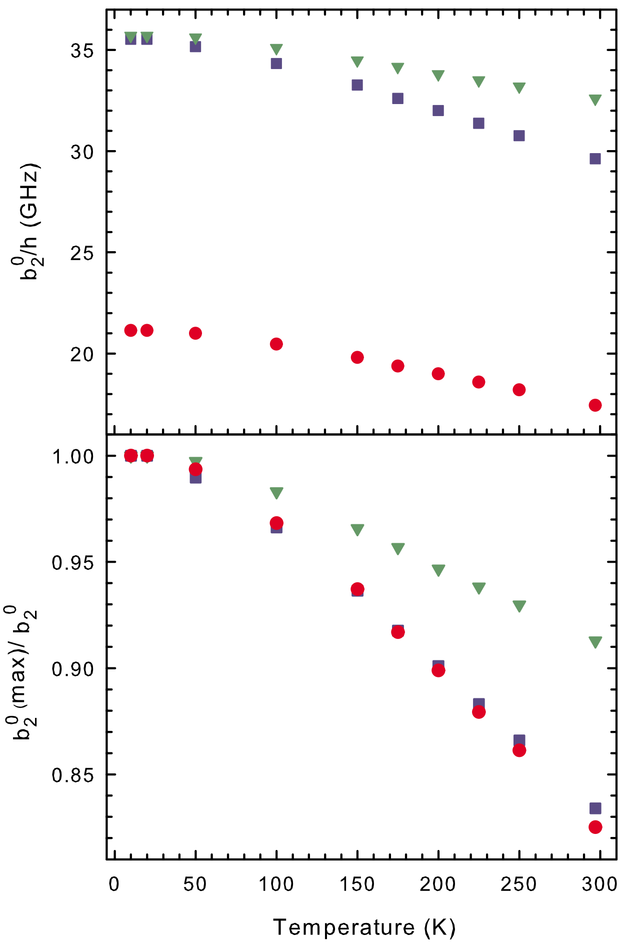

FIG. 7. (Color online) The temperature dependence of the absolute value and fractional change of b_2^0; center 1 (circle), center 2 (square), and center 3 (triangle).

symmetry. Binding to the remaining apical oxygen would likely be required to preserve symmetry; calculations for hydrogen binding to a Fe_{Ti}^{3+}-V_O defect are required. Fluorine is also a candidate impurity, however, the ion charge would be expected to reduce rather than increase the b_2^0 value compared the oxygen vacancy. A third model for center 3 could be a metastable configuration of the Fe_{Ti}^{3+}-V_O defect with closer OII positions and a larger crystal field, possibly involving vacancy formation at the long weak bond position.

The temperature dependence of the SH parameters was also studied, the 20 K roadmap are shown in Figs. 1(c) and 1(d), and detailed parameters given in Table II. The temperature variation of b_2^0/h and of the ratio $b_2^0(\max)/b_2^0$, are shown in Fig. 7. Each center showed a linear increase in b_2^0/h with decreasing temperature down to approximately 50 K, below which the value tended to a constant. Centers 2 and 3 tend to a similar value of ~36 GHz. Comparison of the temperature dependence of the fractional change in the b_2^0 values shows centers 1 and 2 have a similar behavior while center 3 shows a weaker dependence. Comparison of the low-temperature ZFS values found here for centers 2 and 3 with those shown in Table I show them to be the same centers observed by Lewis and Wessel.[13] The variation in b_4^4 found to be less than 10% for all the centers, see Table II and Fig. 1.

IV. CONCLUSIONS

In summary, the presence of two Fe_{Ti}^{3+}-V_O dipole defects in crystal $PbTiO_3$ has been inferred using EPR. It has previously been assumed only one configuration of metal ion oxygen-vacancy defect existed in perovskite oxides. A third Fe^{3+} spectrum has been assigned to the isolated Fe_{Ti}^{3+} defect, the typically low concentration of this center is likely due to the presence of additional acceptor defects. The Fe_{Ti}^{3+}-V_O with the largest zero-field splitting was found to convert to the stable center on annealing, suggesting this is a metastable configuration or that a second impurity ion is bound to the complex in such a way as to preserve tetragonal site symmetry observed by EPR. The measured cubic fourth-order ZFS terms provide insight on the in-plane oxygen positions for the three centers and show these relax outwards for the stable defect dipole.

ACKNOWLEDGMENTS

This work has been partially supported by the Research Councils UK Basic Technology Program (GR/S85726/01).

*d.j.keeble@dundee.ac.uk

[1] G. Arlt and H. Neumann, Ferroelectrics **87**, 109 (1988).
[2] G. E. Pike, W. L. Warren, D. Dimos, B. A. Tuttle, R. Ramesh, J. Lee, V. G. Keramidas, and J. T. Evans, Appl. Phys. Lett. **66**, 484 (1995).
[3] S. Poykko and D. J. Chadi, Phys. Rev. Lett. **83**, 1231 (1999).
[4] D. C. Lupascu and U. Rabe, Phys. Rev. Lett. **89**, 187601 (2002).
[5] X. Ren, Nature Mater. **3**, 91 (2004).
[6] E. S. Kirkpatrick, K. A. Muller, and R. S. Rubins, Phys. Rev. **135**, A86 (1964).
[7] E. Siegel and K. A. Muller, Phys. Rev. B **19**, 109 (1979).
[8] W. L. Warren, D. Dimos, G. E. Pike, K. Vanheusden, and R. Ramesh, Appl. Phys. Lett. **67**, 1689 (1995).
[9] W. L. Warren, G. Pike, K. Vanheusden, D. Dimos, B. Tuttle, and J. Robertson, J. Appl. Phys. **79**, 9250 (1996).
[10] W. L. Warren, B. A. Tuttle, and D. Dimos, Appl. Phys. Lett. **67**, 1426 (1995).
[11] D. J. A. Gainon, Phys. Rev. **134**, A1300 (1964).
[12] R. G. Pontin, E. F. Slade, and D. J. E. Ingram, J. Phys. C **2**, 1146 (1969).
[13] O. Lewis and G. Wessel, Phys. Rev. B **13**, 2742 (1976).
[14] V. V. Laguta, M. D. Glinchuk, I. P. Bykov, Y. L. Maksimenko, J. Rosa, and L. Jastrabik, Phys. Rev. B **54**, 12353 (1996).
[15] H. Meštrić, R.-A. Eichel, K.-P. Dinse, A. Ozarowski, J. van Tol, and L. C. Brunel, J. Appl. Phys. **96**, 7440 (2004).
[16] C. Rudowicz, J. Phys. C **18**, 1415 (1985).
[17] A. Abragam and B. Bleaney, *Electron Paramagnetic Resonance of Transition Ions* (Clarendon Press, Oxford, 1970).

[18] D. G. McGavin, J. Magn. Reson. (1969-1992) **74**, 19 (1987).
[19] Z. Li, M. Grimsditch, X. Xu, and S.-K. Chan, Ferroelectrics **141**, 313 (1993).
[20] S. Stoll and A. Schweiger, J. Magn. Reson. **178**, 42 (2006).
[21] D. J. Newman and W. Urban, Adv. Phys. **24**, 793 (1975).
[22] A. M. Glazer and S. A. Mabud, Acta Crystallogr. B **34**, 1065 (1978).
[23] H. Meštrić, R.-A. Eichel, T. Kloss, K.-P. Dinse, So. Laubach, St. Laubach, P. C. Schmidt, K. A. Schönau, M. Knapp, and H. Ehrenberg, Phys. Rev. B **71**, 134109 (2005).
[24] C. H. Park and D. J. Chadi, Phys. Rev. Lett. **84**, 4717 (2000).
[25] W. Low, Phys. Rev. **105**, 792 (1957).
[26] K. A. Muller, Helv. Phys. Acta **31**, 173 (1958).